Single tapered fiber tip for simultaneous measurements of thickness, refractive index and distance to a sample

Carlos Moreno-Hernández,[1] David Monzón-Hernández,[1,*] Iván Hernández-Romano,[1] and Joel Villatoro[2,3]

[1]*Centro de Investigaciones en Óptica, Loma del Bosque 115, Colonia Lomas del Campestre, León, Guanajuato 37150, Mexico*

[2]*Dept. of Communications Engineering, Escuela Técnica Superior de Ingeniería (ETSI) de Bilbao. University of the Basque Country (UPV/EHU), Alda. Urquijo s/n, E-48013 Bilbao, Spain*

[3]*IKERBASQUE –Basque Foundation for Science, E-48011 Bilbao, Spain*

[*]*dmonzon@cio.mx*

Abstract: We demonstrate the capability of an air cavity Fabry-Perot interferometer (FPI), built with a tapered lead-in fiber tip, to measure three parameters simultaneously, distance, group refractive index and thickness of transparent samples introduced in the cavity. Tapering the lead-in fiber enhances the light coupling back efficiency, therefore is possible to enlarge the air cavity without a significant deterioration of the fringe visibility. Fourier transformation, used to analyze the reflected optical spectrum of our FPI, simplify the calculus to determine the position, thickness and refractive index. Samples made of 7 different glasses; fused silica, BK7, BalF5, SF2, BaF51, SF15, and glass slides were used to test our FPI. Each sample was measured nine times and the results for position, thickness and refractive index showed differences of ± 0.7%, ± 0.1%, and ± 0.16% respectively. The evolution of thickness and refractive index of a block of polydimethylsiloxane (PDMS) elastomer due to temperature changes in the range of 25°C to 90°C were also measured. The coefficients of the thermal expansion and thermo-optic estimated were $\alpha = 4.71 \times 10^{-4}$/°C and $dn/dT = -4.66 \times 10^{-4}$ RIU/°C, respectively.

OCIS codes: (060.2370) Fiber optics sensors; (120.2230) Fabry-Perot; (120.3180) Interferometry; (160.4760) Optical properties; (280.4788) Optical sensing and sensors.

References and links

1. V. Bhatia, K. A. Murphy, R. O. Claus, M. E. Jones, J. L. Grace, T. A. Tran, and J. A. Greene, "Optical fibre based absolute extrinsic Fabry–Perot interferometric sensing system," Meas. Sci. Technol. **7**(1), 58–61 (1996).
2. V. Arya, M. de Vries, K. A. Murphy, A. Wang, and R. O. Claus, "Exact analysis of the extrinsic Fabry-Perot interferometric optical fiber sensor using Kirchhoff's diffraction formalism," Opt. Fiber Technol. **1**(4), 380–384 (1995).
3. X. Wen, T. Ning, Y. Bai, C. Li, J. Li, and C. Zhang, "Ultrasensitive temperature fiber sensor based on Fabry-Pérot interferometer assisted with iron V-groove," Opt. Express **23**(9), 11526–11536 (2015).
4. T. Wang, S. Zheng, and Z. Yang, "A high precision displacement sensor using a low-finesse fiber-optic Fabry–Pérot interferometer," Sens. Actuators A Phys. **69**(2), 134–138 (1998).
5. K. Thurner, P. F. Braun, and K. Karrai, "Fabry-Pérot interferometry for long range displacement sensing," Rev. Sci. Instrum. **84**(9), 095005 (2013).
6. W. Wang and F. Li, "Large-range liquid level sensor based on an optical fibre extrinsic Fabry–Perot interferometer," Opt. Lasers Eng. **52**, 201–205 (2014).
7. G. Zhang, M. Yang, and Y. Wang, "Optical fiber-tip Fabry–Perot interferometer for hydrogen sensing," Opt. Commun. **329**, 34–37 (2014).
8. R. Wang and X. Qiao, "Gas refractometer based on optical fiber extrinsic Fabry-Perot interferometer with open cavity," IEEE Photonics Technol. Lett. **27**(3), 245–248 (2015).
9. G. Liu, M. Han, and W. Hou, "High-resolution and fast-response fiber-optic temperature sensor using silicon Fabry-Pérot cavity," Opt. Express **23**(6), 7237–7247 (2015).

#246295 Received 27 Jul 2015; accepted 5 Aug 2015; published 13 Aug 2015

10. C. J. Moreno-Hernández, D. Monzón-Hernández, A. Martínez-Ríos, D. Moreno-Hernández, and J. Villatoro, "Long-range interferometric displacement sensing with tapered optical fiber tips," IEEE Photonics Technol. Lett. **27**(4), 379–382 (2015).
11. W. Wang, N. Wu, Y. Tian, X. Wang, C. Niezrecki, and J. Chen, "Optical pressure/acoustic sensor with precise Fabry-Perot cavity length control using angle polished fiber," Opt. Express **17**(19), 16613–16618 (2009).
12. R. Wang and X. Qiao, "Hybrid optical fiber Fabry-Perot interferometer for simultaneous measurement of gas refractive index and temperature," Appl. Opt. **53**(32), 7724–7728 (2014).
13. S. Pevec and D. Donlagic, "High resolution, all-fiber, micro-machined sensor for simultaneous measurement of refractive index and temperature," Opt. Express **22**(13), 16241–16253 (2014).
14. W. V. Sorin and D. F. Gray, "Simultaneous thickness and group index measurement using optical low-coherence reflectometry," IEEE Photonics Technol. Lett. **4**(1), 105–107 (1992).
15. G. J. Tearney, M. E. Brezinski, J. F. Southern, B. E. Bouma, M. R. Hee, and J. G. Fujimoto, "Determination of the refractive index of highly scattering human tissue by optical coherence tomography," Opt. Lett. **20**(21), 2258–2260 (1995).
16. T. Fukano and I. Yamaguchi, "Simultaneous measurement of thicknesses and refractive indices of multiple layers by a low-coherence confocal interference microscope," Opt. Lett. **21**(23), 1942–1944 (1996).
17. S. R. Chinn, E. A. Swanson, and J. G. Fujimoto, "Optical coherence tomography using a frequency-tunable optical source," Opt. Lett. **22**(5), 340–342 (1997).
18. J. H. Chen, J. R. Zhao, X. G. Huang, and Z. J. Huang, "Extrinsic fiber-optic Fabry-Perot interferometer sensor for refractive index measurement of optical glass," Appl. Opt. **49**(29), 5592–5596 (2010).
19. H. C. Cheng and Y. C. Liu, "Simultaneous measurement of group refractive index and thickness of optical samples using optical coherence tomography," Appl. Opt. **49**(5), 790–797 (2010).
20. I. K. Ilev, R. W. Waynant, K. R. Byrnes, and J. J. Anders, "Dual-confocal fiber-optic method for absolute measurement of refractive index and thickness of optically transparent media," Opt. Lett. **27**(19), 1693–1695 (2002).
21. X. Wang, C. Zhang, L. Zhang, L. Xue, and J. Tian, "Simultaneous refractive index and thickness measurements of bio tissue by optical coherence tomography," J. Biomed. Opt. **7**(4), 628–632 (2002).
22. T. Fukano and I. Yamaguchi, "Separation of measurement of the refractive index and the geometrical thickness by use of a wavelength-scanning interferometer with a confocal microscope," Appl. Opt. **38**(19), 4065–4073 (1999).
23. J. Na, H. Y. Choi, E. S. Choi, C. Lee, and B. H. Lee, "Self-referenced spectral interferometry for simultaneous measurements of thickness and refractive index," Appl. Opt. **48**(13), 2461–2467 (2009).
24. S. Kim, J. Na, M. J. Kim, and B. H. Lee, "Simultaneous measurement of refractive index and thickness by combining low-coherence interferometry and confocal optics," Opt. Express **16**(8), 5516–5526 (2008).
25. S. C. Zilio, "Simultaneous thickness and group index measurement with a single arm low-coherence interferometer," Opt. Express **22**(22), 27392–27397 (2014).
26. R. Keil, E. Klement, K. Mathyssek, and J. Wittmann, "Experimental investigation of the beam spot size radius in single-mode fibre tapers," Electron. Lett. **20**(15), 621–622 (1984).
27. S. W. Harun, K. S. Lim, C. K. Tio, K. Dimyati, and H. Ahmad, "Theoretical analysis and fabrication of tapered fiber," Optik (Stuttg.) **124**(6), 538–543 (2013).
28. Y. Zhang, Y. Li, T. Wei, X. Lan, Y. Huang, G. Chen, and H. Xiao, "Fringe visibility enhanced extrinsic Fabry-Perot interferometer using a graded index fiber collimator," IEEE Photonics J. **2**(3), 469–481 (2010).
29. K. P. Jedrzejewski, F. Martinez, J. D. Minelly, C. D. Hussey, and F. P. Payne, "Tapered-beam expander for single-mode optical-fibre gap devices," Electron. Lett. **22**(2), 105–106 (1986).
30. C. Markos, K. Vlachos, and G. Kakarantzas, "Bending loss and thermo-optic effect of a hybrid PDMS/silica photonic crystal fiber," Opt. Express **18**(23), 24344–24351 (2010).

1. Introduction

The Fabry-Perot interferometer (FPI) is one of the simplest optical fiber interferometers as it can be built with just a cleaved optical fiber separated from a reflecting surface [1–3]. Due to the high divergence of the output beam of the optical fiber the separation between the fiber facet and the reflecting surface is limited to a few hundred micrometers [2] which can be sufficient for some sensing applications. The majority of extrinsic fiber FPIs reported in the literature so far are capable of monitoring a single parameter only [3–10]. However, it is possible to micro-machine the fiber that forms a FPI to make it capable of monitoring or sensing two parameters, see for example [11–13]. The disadvantage in the latter case is the multistep process needed to machine the optical fiber tip.

Another limitation of most extrinsic FPIs reported until now is the fact that the performance of the interferometer can be compromised with residues of liquids or polymers left on the facet of the optical fiber. Contamination of the fiber tip will perturb the reference beam, and consequently, the performance of the interferometer. In many sensing architectures

#246295 Received 27 Jul 2015; accepted 5 Aug 2015; published 13 Aug 2015

reported until now the end of the optical fiber that forms the FPI cannot be completely isolated, particularly in those designed to measure refractive index of liquids. Such measurement is crucial in a number of industrial processes, analytical chemistry or bio-medical analysis. A number of schemes based on optical fibers had been proposed to measure refractive index of solid, liquids, or gases. In the latter two cases, typically the optical fiber is in immersed into the sample under test [12,13]. By contrast, for the measurement of refractive index of solid samples the use of non-contact approaches based on interferometry are widely extended. Most of these schemes are capable to measure the group refractive index (n_g) and geometrical thickness (t) simultaneously [14–25]. The majority of the aforementioned methods use optical fibers to carry and collect the probe beam. Since the beam exiting the fiber rapidly diverges, thus collimating lenses are necessary. Precise translation mounts are also necessary to adjust the lenses and mirrors position [14–16]. A practical alternative to transport and collect a probe beam is by means of low cost beam expanders based on a single mode tapered fiber tip [24,25]. Such tips can be made by stretching a single mode fiber while it is heated. The process should fulfill the conditions to accomplish the adiabaticity criteria [26,27], to avoid the excitation of other modes than the fundamental.

Here, we report on an extrinsic FPI built with an optical fiber tip, tapered to a proper diameter, to measure simultaneously the distance (respect to a fiber tip), thickness, and refractive index of a solid dielectric sample. The fiber tip plays a triple role in the interferometer; it provides the reference beam for the FPI, minimizes the divergence of the output beam and couples more efficiently the reflected light [10]. By analyzing the Fourier domain reflection spectra of the FPI, as widely explained in [13,14,25], it is possible to stablish simple relationships to calculate the n_g and t of the sample under test. We also demonstrate that using this interferometer it is possible to measure in real-time the changes in the thickness and RI of a polymer block due to temperature changes. With this information we could determine the coefficient of the thermal expansion (CTE) and thermo-optic coefficient (TOC) of the block. An important advantage of our interferometer is that it can be used to test samples composed by a stack of layers of different refractive indices and thicknesses. We take advantage of this capability to demonstrate the in-depth layer profiling, using a sample with an air cavity inside. Our configuration offers the possibility of scanning and multiplexing.

2. Tapered fiber tip interferometer

The basic structure of an extrinsic fiber Fabry-Perot interferometer consists of a lead-in fiber in front of a reflecting surface. Some approaches have been proposed to increase the FPI cavity without losing fringe visibility, see for example [5,10,14,28]. FPIs with long cavities make possible to introduce small dielectric blocks in them, hence it is possible to measure parameters like thickness or refractive index or even profiling one or both surfaces of a sample. Tapering the lead-in optical fiber of an extrinsic FPI had been proved to enhance its fringe visibility [10]. Under some tapering conditions, the mode field diameter (MFD) of the lead-in tapered tip increases compared to that of an un-tapered fiber, as can be seen in Fig. 1(a). But the most important effect is the reduction of the divergence of the output beam [26,29], which enhances the coupling back-in of the reflected light, allowing to increase the air cavity length of a FPI. Fiber tapers with a waist diameter of 55 μm were fabricated in a glass processing system (Vytran, GPX-3100). Then, they were cleaved at the middle of the waist length to obtain two useful tapered fiber tips, the process is described in detail in [10]. Then the un-tapered end of the lead-in fiber tip was connected to an optical sensing interrogator (sm125, Micron Optics) that consists of a tunable laser with a bandwidth from 1510 to 1590 nm synchronized with an internal photodetector. When a reflecting surface is placed to a distance L in front of the lead-in tapered fiber tip the interference between two beams occurs [1–5]. A representation of the set-up used to analyze the interference spectra generated in the FPI is shown in Fig. 1(b).

#246295 Received 27 Jul 2015; accepted 5 Aug 2015; published 13 Aug 2015

The back-reflected optical spectrum of the fiber FPI is shown in Fig. 2(a), the characteristics of these spectra such as period and visibility mainly depends on the air-cavity length. The analysis of this type of interference pattern in the Fourier domain has been broadly studied [13,14,25]. This is a very simple method to measure the distance between the fiber tip and an object; as can be seen in Fig. 2(b), where the FFT modulus peaks can be directly related with the cavity length.

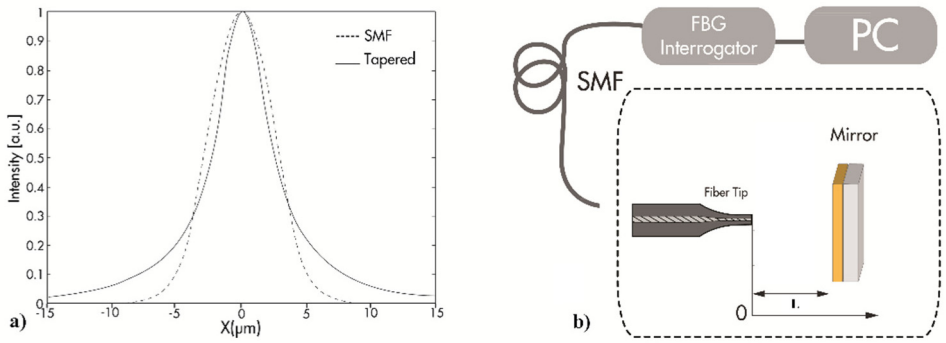

Fig. 1. (a) Calculated mode MFD of the fundamental mode: of a SM fiber (dashed line) and a SM fiber tapered to 55 μm (continuous line), (b) Representation of the experimental set-up used to interrogate the FFPI.

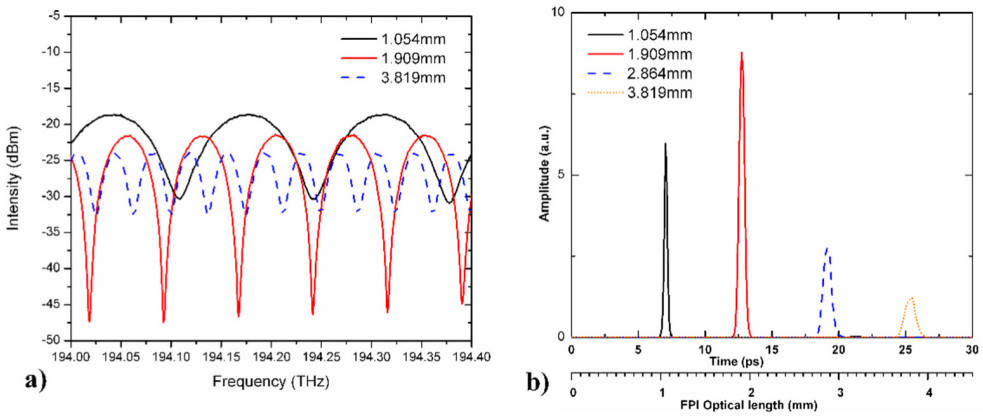

Fig. 2. (a) Reflection spectra of the extrinsic tapered FFPI for three different cavity lengths, (b) Calculated FFT modulus of the reflection spectra of the interferometer with four different cavity lengths.

Based on the above principle we established a method to measure the geometrical thickness and group refractive index of dielectric samples, glasses and polymers, using the tapered fiber FPI. Firstly, we obtain the interference spectra when fiber tip and mirror were separated a distance L. In the Fourier domain a single peak was obtained, as shown in Fig. 2 (b) the second X-axis in the FFT graph indicates the separation of the mirror from the fiber tip in millimeters. This separation was labeled as X_3, following the same nomenclature used by Sorin and Gray in [14]. When a dielectric sample, a block of SF-15 glass for example, is introduced in the cavity of the tapered fiber FPI, as is depicted in Fig. 3(a), the optical path between the fiber and mirror increases, and also the OPD of the interference. But the most important thing is that the presence of two new interfaces will transform the two-beam interference into a four-beam interference. The back-reflected spectra will exhibit the superposition of several modulated signals (graphs in Fig. 3(b)). The Fourier domain spectra

#246295 Received 27 Jul 2015; accepted 5 Aug 2015; published 13 Aug 2015

exhibits three peaks (graph of Fig. 3(c)). By analyzing the position of the three peaks it is possible to know the corresponding length for each optical path (L_i) along the axis. The original peak position of the mirror (X_3) moved to the right to a new position in Fourier domain, labeled as X_4 (due to the insertion of the sample). Two more peaks appear, X_1 and X_2, which represent the distance from the fiber tip to the closest and furthest faces of the dielectric sample, respectively. Based on the analysis reported in [14] the optical path difference introduced by the dielectric sample is

$$OPD = X_2 - X_1 \tag{2}$$

The thickness of the sample, in mm, can be calculated from the frequency peak position through

$$t = OPD - (X_4 - X_3) \tag{3}$$

Since OPD is equal to the product $n_g * t$ it is possible to determine the group refractive index of the sample,

$$n_g = \frac{OPD}{t} \tag{4}$$

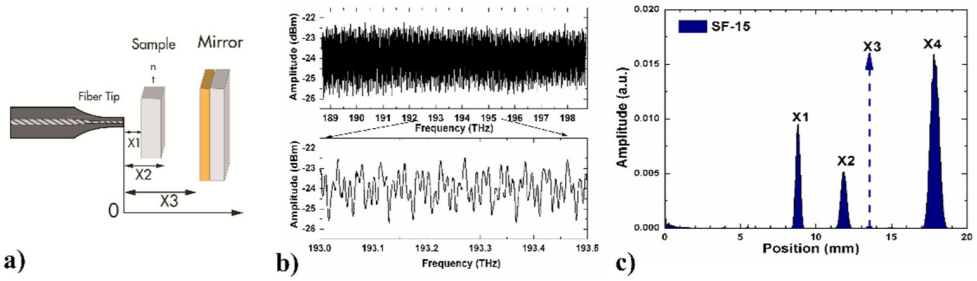

Fig. 3. (a) Schematic diagram that shows the disposition of the elements for samples measurement, (b) Optical spectrum of the SF-15 sample and mirror. (c) FFT of the optical spectrum showing the relation between peak position and distances from the fiber tip.

3. Results and discussion

Using the setup shown in Fig. 1(b), the fiber tip was mounted in a linear translation stage (NanoMax-343M/Thorlabs) and it was moved away from the mirror surface starting at 100μm until 3000μm in steps of 100μm. The reflected spectra of the tapered FPI was used to calculate the cavity lengths. The maximum difference resulted between the calculated value and the stage position was ± 0.7%, but this combines the error from the stage and the calculated cavity. To complete our study five round transparent glass windows, of 25 mm in diameter and approximately 1.8 mm of width were fabricated in our facilities. They were made of fused silica, Schott glasses: BK-7, BaLF-5, SF-2 and SF-15. We also used a glass slide and a glass cover made by Corning. Following the procedure described above we measured geometrical thickness and the group refractive index of the samples, the values obtained are shown in Table 1. Each value in the table represents the average of the 9 measurements we got for two samples of each type in a range from 4 to 8 mm from the fiber tip with steps of 0.5mm.

#246295 Received 27 Jul 2015; accepted 5 Aug 2015; published 13 Aug 2015

Table 1. Results for thickness measurement where we compared our method with the micrometer measures. Results for group refractive index measurements obtained with the method proposed compared to the theoretical ng at l = 1550nm.

Glass	Thickness (mm)			Group refractive index		
	sample	reference	%error	sample	reference	%error
Silica	1.8088	1.809	0.025	1.464	1.4626	0.105
BK-7	1.8074	1.808	0.059	1.520	1.5201	0.006
BALF-5	1.7964	1.797	0.060	1.547	1.5488	0.157
SF-2	1.7686	1.769	0.045	1.642	1.6424	0.042
BAF-51	1.8231	1.823	0.012	1.648	1.6490	0.080
SF-15	1.7959	1.796	0.010	1.689	1.6909	0.165
Cover	0.1941	0.194	0.01	1.5186	-	-
Slide	1.1481	1.148	0.01	1.5126	-	-

It can be seen in the table that the error of the thickness measurements is lower than 0.1%, and the lowest thickness error corresponded to the SF-15 sample with 0.010%. Uncertainties can be caused by the different surface finishes that each sample presents because they were polished in batch regardless of the hardness of each type of glass. Also we found that when the OPD of the sample was larger the error decreased in thickness and group refractive index measurement. We used SF-15 sample to study the variations of t and n_g measurements compared to the reference values at different distances from fiber tip. In Fig. 4(a) the results are shown, it can be seen that for a distance larger than 5 mm the difference between the measured and reference values start to increase but even in such cases the error is lower than that reported in literature using other methods [24,25]. In the right graph of Fig. 4(b), the measurement behavior through a finite period of time is shown, the variations are less than $1x10^{-4}$ RI units.

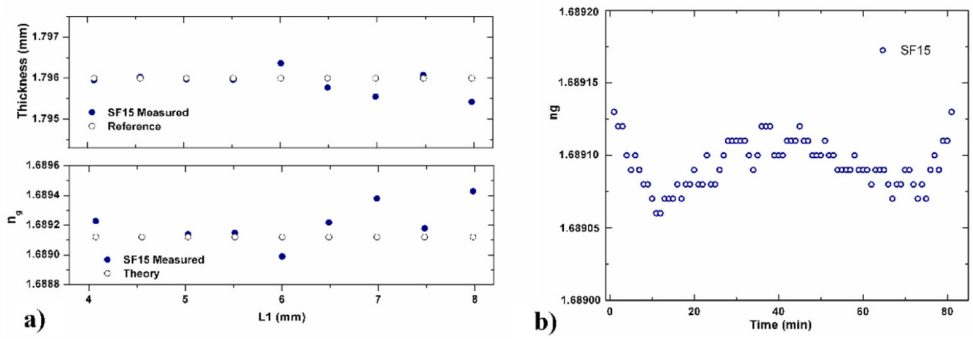

Fig. 4. Results obtained with SF-15 glass sample. (a) Measurements of t and ng when glass is at different separation from the fiber tip. (b) The measurement of ng at a fixed distance during 80 minutes that shows the variations of the ng value due to temperature and/or vibrations.

3.1. CTE and dn/dT simultaneous measurements

An application of the proposed tapered fiber FPI is to measure dynamic changes of t and n_g of different dielectric samples. For example, the thickness and index of some polymers with high sensitivity to temperature change. We prepared a rectangular block of polydimethylsiloxane (PDMS) elastomer (Dow Corning- Sylgard 184). The two part liquid components were mixed and then they were put inside a glass container formed with glass slides, after it was cured the

#246295 Received 27 Jul 2015; accepted 5 Aug 2015; published 13 Aug 2015

container was disassembled to obtain a rectangular polymer prism as shown in Fig. 5(a). A gold film mirror, in direct contact with the PDMS was used as a reference surface. First, the fiber was placed in position 1, aside the polymer, to obtain the reference peak, the corresponding peaks are shown in Fig. 5(b). Then, the fiber was moved to position 2 as shown in Fig. 5(a) over the polymer. The new peak positions were saved, and by using Eqs. (2) to (4) it is possible to find that the polymer thickness = X_{REF}-X_1 = 11.745 mm and n_g = (X_2-X_1)/thickness = 1.3983. This refractive index value is close enough to the one reported by the manufacturer of 1.3997 at 1554nm at 25°C.

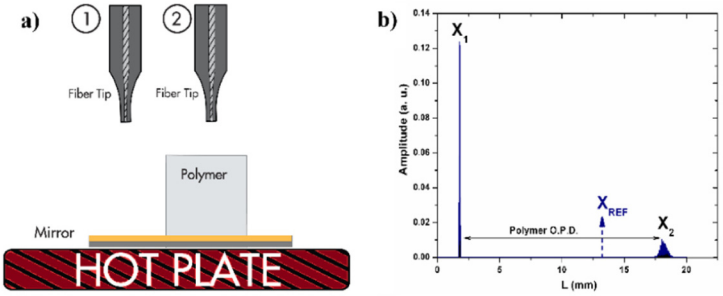

Fig. 5. (a) Scheme of the setup that shows the polymer sample in the container and tapered fiber tip. (b). Fourier domain interference peak positions obtained for measuring the group refractive index and thickness.

It is known that PDMS has a large thermo-optic coefficient, this allowed us to study the capacity of our interferometer to measure dynamic changes of the refractive index. Also this can be used to calculate resolution of the system to measure the refractive index. We heated the sample and measured the t and n_g values as the temperature changed. We began to heat the sample from 25 to 90°C while saving the positions of the FFT maximum peaks (X_1, X_2, and X_{REF}). Using the relations described above we could know the thickness and refractive index of the elastomer at different temperatures. In Fig. 6 the results are shown, a linear change of t and n_g due to temperature change resulted in $\alpha = 4.71\text{x}10^{-4}$ /°C for linear expansion and $dn/dT = -4.67\text{x}10^{-4}$ RIU/°C, respectively. The latter value agrees well with the thermo-optic coefficient of the elastomer reported in [30]. Since polymer was not comprised in a container it was possible to stablish that this change of the geometrical thickness measured is the actual thermal expansion coefficient.

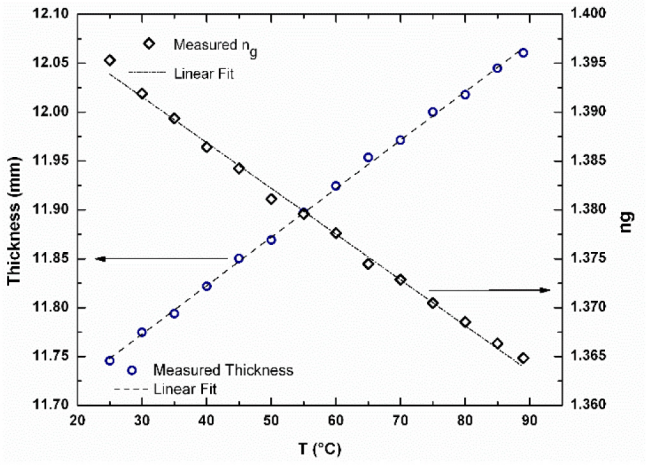

Fig. 6. Plotted results of Sylgard 184 temperature vs. thickness and RI behavior due to the temperature change.

#246295 Received 27 Jul 2015; accepted 5 Aug 2015; published 13 Aug 2015

Although, we have just measured the n_g and t along one axis of the samples under test, the small dimensions of the interrogation beam allow us to carry out measurements in the 3 axis of a sample.

4. Conclusions

A simple and versatile extrinsic fiber FPI is reported. The tapered fiber minimizes the divergence of the output beam of the optical fiber and couples the reflected light more efficiently than an un-tapered optical fiber. As a result, extrinsic FPIs with long cavities can be implemented which allow the insertion of thick samples inside the cavity. We demonstrated that our FPI can be used to measure simultaneously, group refractive index and thickness of a sample as well as distance to the sample. Differences between our measurements and the actual values are less than 0.16% for the three measurements. The simultaneous measurements performed with the PDMS sample to obtain dn/dT coefficient present a difference of $1x10^{-5}$ RIU compared with previous reported value. On the other hand the result for the coefficient of linear expansion (α) presents a difference of $1.7x10^{-4}$ compared to the value provided by the manufacturer.

The interferometer here reported has several important advantages including flexibility, miniature size and multiplexing capability among others. We have demonstrated that our FPI can simplify the measurements of CTE or dn/dT of some materials.

Acknowledgments

The work by C. Moreno-Hernández and I. Hernández-Romano was supported by the Mexican Council for Science and Technology (CONACYT) with a PhD and Postdoctoral fellowship, respectively. D. Monzón-Hernández and J. Villatoro are also grateful to CONACYT for the "Estancias de Consolidación" Project under Grant 217697.